www.czasopisma.pan.pl PAN POLSKA AKADEMIA NAUK www.journals.pan.pl

Arch. Min. Sci. **65** (2020), 1, 159-178

Electronic version (in color) of this paper is available: http://mining.archives.pl

DOI 10.24425/ams.2020.132713

WEI ZHANG[1,2], JIA-JIA TANG[2], DONG-SHENG ZHANG[1,2]*,
LEI ZHANG[2], YUYAN SUN[2], WEI-SHENG ZHANG[2]

EXPERIMENTAL STUDY ON THE JOINT APPLICATION OF INNOVATIVE TECHNIQUES FOR THE IMPROVED DRIVAGE OF ROADWAYS AT DEPTHS OVER 1 KM: A CASE STUDY

Finding effective ways to efficiently drive roadways at depths over 1 km has become a hotspot research issue in the field of mining engineering. In this study, based on the local geological conditions in the Xinwen Mining Area (XMA) of China, in-situ stress measurements were conducted in 15 representative deep roadways, which revealed the overall tectonic stress field pattern, with the domination of the horizontal principal stresses. The latter values reached as high as 42.19 MPa, posing a significant challenge to the drivage work. Given this, a comprehensive set of innovative techniques for efficiently driving roadways at depths over 1 km was developed, including (i) controlled blasting with bidirectional energy focusing for directional fracturing, (ii) controlled blasting with multidirectional energy distribution for efficient rock fragmentation, (iii) wedge-cylinder duplex cuts centered on double empty holes, and (iv) high-strength supports for deep roadways. The proposed set of techniques was successfully implemented in the –1010 west rock roadway (WRR) drivage at the Huafeng Coal Mine (HCM). The improved drivage efficiency was characterized by the average and maximum monthly advances of 125 and 151 m, respectively. The roadway cross-sectional shape accuracy was also significantly improved, with the overbreak and underbreak zones being less than 50 mm. The deformation in the surrounding rock of roadway (SRR) was adequately controlled, thus avoiding repeated maintenance and repair. The relevant research results can provide technical guidance for efficient drivage of roadways at depths over 1 km in other mining areas in China and worldwide.

Keywords: roadways at depth over 1 km, in-situ stress measurements, efficient drivage, rapid drilling and blasting, deformation control of SRR, industrial test

[1] CHINA UNIVERSITY OF MINING AND TECHNOLOGY, STATE KEY LABORATORY OF COAL RESOURCES AND SAFE MINING, XUZHOU 221116, CHINA
[2] CHINA UNIVERSITY OF MINING AND TECHNOLOGY, SCHOOL OF MINES, XUZHOU 221116, CHINA

* Corresponding Author:dshzhang123@cumt.edu.cn

1. Introduction

Deep mining and driving are challenging issues for mining engineers worldwide. Insofar as the depth, to which the mine can be operated economically, depends on the market value of the ore extracted, the deepest mines (2-4 km of depth) are golden ones, which are mostly located in South Africa (Fairhurst, 2017). In contrast, the prevailing majority of coal mines worldwide are shallower than 1 km. In particular, the coal mines in China deeper than 600 m account for 28.5% of the coal production (Kulatilake et al., 2013), while the number of coal mines deeper than 1 km has recently exceeded 45 (Luo et al., 2014), the largest mining depth having surpassed 1.3 km (Kang, 2014). However, under the strict control of the development of replacement coal mines at the policy level in China (Blondeel & Van, 2018), most existing coal mines have successively begun deep mining to ease the shortage of replacement mines. Given the current mining rates, the coal mines across China are extending downward at rates of 8-12 m per year. Especially, eastern coal mines are descending more rapidly at speeds of 10-25 m per year (Kang, 2014). It is expected that many coal mines in China will exceed the depth range of 1 km in the next two decades. However, there are serious technical difficulties in mining at depths over 1 km (Diering, 1997; Hu & Dong, 2008; Ranjith et al., 2017), severely impeding the safety and efficiency of underground mining. Insofar as the underground forces acting on the coal-rock masses surrounding the roadway or mine increase with depth, possible depth limits to which coal can be mined economically must include a consideration of the ability to excavate the rock and maintain serviceable workings for as long as required (Fairhurst, 2017).

Noteworthy is that the *13th Five-Year (2016-2020) Plan for the Development of the Coal Industry* in China envisages the optimization of coal production structure in the western part of China, with its limitation in the eastern, central, and northeastern regions (Qi et al., 2016; Zhang et al., 2018). In this context, the present study analyzed the difficulties and breakthrough solutions for excavating deep roadways in the XMA, which is located in central and western Shandong province, covers an area of 912 km^2, and is among the oldest mining areas with considerable mining depths in China. All mines within this area have already entered the stage of deep mining, with an average mining depth of 1.032 km, and most mines are more than 1.2 km in mining depth (around 1.5 km maximum). Deep mining in the XMA is characterized by elevated in-situ stresses, ground temperatures, and karst water pressures, which exert intense disturbance to the surrounding rock (He et al., 2005). The local coal mines undergo a transition from quantitative changes to qualitative ones in the occurrence of mining hazards, making the underground mining and excavating extremely difficult. Roadways excavated in the XMA each year have a total length of over 200 km, about 70% of which correspond to complex conditions and considerable depths (Ma et al., 2009). On the one hand, as the mining depth increases annually, development works have to extend downward continually, and the surrounding rock conditions deteriorate with depth. On the other hand, deep roadways need to have large cross-sections for improved ventilation (Sasmito et al., 2013), which adds to the difficulty of their excavation.

Upon the roadway depth exceeding 1 km, the SRR undergoes very high levels of concentrated and deviatoric stresses due to the high in-situ stresses in deep coal-rock masses after the roadways excavation (Malan & Basson, 1998; Zhang, 2017; Qi et al., 2009), which is fundamentally different from the conditions of shallow depths. The deformation and failure of deep SRR are typically characterized by plastic flow, dilatancy, and discontinuity (Chang & Xie, 2009; Agliard et al., 2001; Li et al., 2015), presenting a severe challenge to the roadway drivage at deep levels. Two main approaches are widely used to tackle these problems, namely (1) drilling and blasting

method, and (2) fully-mechanized excavation method (Cai, 2011; Zhang et al., 2011; Rautenstrauch & Kulassek, 2014; Li et al., 2017; Yang, 2013; Huang et al., 2018; Zheng et al., 2016). However, the implementation of these approaches to the particular roadway projects requires a comprehensive analysis of local mining geological conditions. Given this, the local mining geological conditions and the in-situ stress measurements from existing deep roadways in the XMA were analyzed in this study, and a set of breakthrough techniques for efficiently excavating roadways at depths over 1 km was successfully developed and applied to excavate the -1010 WRR at the HCM, XMA. These techniques and their implementation schemes are discussed in detail in the following sections of this paper, while the basic conclusions on the significant improvement of the driving efficiency and cross-sectional shape are proved by the experimental results on the efficient excavation of roadways deeper than 1 km.

2. Problems encountered in the deep roadways excavation in the XMA

During coal mining and other engineering activities at underground mines, the deformation and failure of coal-rock masses are mainly controlled by in-situ stresses (Martin et al., 2003; Cai & Peng, 2011). Therefore, the knowledge of in-situ stress distribution in the coal-rock masses in the study area is necessary for the theoretical substantiation of underground mine works and respective decision-making (Sato et al., 2000; Chen et al., 2017; Lavrov, 2003) on such issues as roadway site selection, determination of support parameters, roof control, and prevention and control of mining-related hazards. To this end, an in-situ stress measurement system by small-borehole hydraulic fracturing (SYY-56, China Coal Research Institute, Beijing, China) (Kang et al., 2010; Kang, 2007), was applied in 15 representative roadways deeper than 1 km at the Panxi Coal Mine (PCM), Suncun Coal Mine (SCM), Huafeng Coal Mine (HCM), and Xiezhuang Coal Mine (XCM) within the XMA. The measurement results for each particular roadway are listed in table 1, where D is the burial depth of roadway; σ_V is vertical principal stress; $\sigma_{H\max}$ and $\sigma_{H\min}$ are maximum and minimum horizontal principal stresses, respectively; α denotes the direction of maximum horizontal principal stress; k_1 is the ratio of the maximum horizontal principal stress to the vertical one; k_2 is the ratio of the minimum horizontal principal stress to the vertical one; and k_3 is the maximum-to-minimum ratio of horizontal principal stresses. The analysis of the above measurements revealed the following patterns.

(1) The depth of 15 representative measurement sites ranges between 1,001 and 1,342 m, which implies high in-situ stresses in the SRR. In ten measurement sites of the total fifteen (i.e., in about 66.7% cases), the vertical principal stresses exceeded 30 MPa, their maximum value being 33.55 MPa. Such a high level of in-situ stresses is more strict requirements to the support equipment, as well as blasting and drilling parameters and techniques.

(2) The SRR in high-stress conditions are subjected to more intense disturbance from underground mining and, thus, are prone to the large-scale inelastic deformation. To minimize the latter and attain a higher bearing capacity, it is expedient to arrange roadways preferably through hard rock strata, which will inevitably deteriorate the mining advance and driving efficiency parameters.

(3) In ten measurement sites (i.e., about 66.7% cases), the maximum horizontal principal stress exceeded the vertical one. In the remaining five sites (two roadways in the SCM and three ones in the HCM), the maximum horizontal principal stresses were slightly lower than verti-

TABLE 1

In-situ stress measurement results from 15 representative deep roadways in the XMA

No.	Name	Site	D/m	σ_V/ MPa	$\sigma_{H\max}$/ MPa	$\sigma_{H\min}$/ MPa	α	k_1	k_2	k_3
1	PCM	–1100 west main roadway	1,342	33.55	33.94	17.49	N57.3°E	1.012	0.521	1.941
2	PCM	7192 tailgate chamber	1,001	25.84	29.65	11.03	N43.8°E	1.147	0.427	2.688
3	SCM	–1050 west main roadway	1,283	32.08	31.97	16.51	N6.0°E	0.997	0.515	1.936
4	SCM	2421 tailgate	1,034	25.85	23.22	12.19	N35.0°E	0.898	0.472	1.905
5	SCM	–1100 main roadway of district #1	1,251	31.28	35.67	18.54	N39.9°W	1.140	0.593	1.924
6	SCM	–1100 main dip of district #2	1,259	31.48	35.82	19.05	N16.9°E	1.138	0.605	1.880
7	SCM	–1100 main dip of district #3	1,271	31.78	39.13	21.03	N11.3°E	1.231	0.662	1.861
8	HCM	–920 level cross-cut	1,040	27.66	31.35	16.20	N23.5°W	1.133	0.586	1.935
9	HCM	–1010 level main roadway	1,130	29.95	35.15	19.10	N31.5°E	1.174	0.638	1.840
10	HCM	–1100 main haulage roadway	1,220	32.33	42.19	22.80	N3°E	1.305	0.705	1.850
11	HCM	–1180 main return roadway (left end)	1,274	31.85	29.34	14.74	N60.7°E	0.921	0.463	1.991
12	HCM	–1180 main return roadway (right end)	1,274	31.85	30.19	16.82	N46.8°E	0.948	0.528	1.795
13	HCM	–1180 subinclined shaft chamber	1,271	31.78	31.19	16.74	N67.7°E	0.981	0.527	1.863
14	XCM	–850 main dip of district #2	1,071	28.38	39.77	20.64	N39.7°E	1.401	0.727	1.927
15	XCM	1202 east headgate	1,150	30.48	34.60	17.89	N12.5°E	1.135	0.587	1.934

cal ones, with the difference not exceeding 2.63 MPa. The maximum horizontal principal stresses over 30 MPa were observed in 12 sites (80% cases), the largest value of 42.19 MPa being revealed in the HCM (site #10). Thus, the in-situ stresses for the sites under the study are dominated by horizontal stresses, which pattern is typical of a tectonic stress field. Under such conditions, conventional excavation methods are considered quite ineffective.

(4) The high in-situ stresses observed at mining depths over 1 km, combined with the complex geologic structure of deep strata, are likely to cause the failure of both the primary support and secondary reinforced support for the SRR. In some cases, the stability of SRR remains problematic due to large-scale and long-term deformation even after the implementation of additional support and repair measures. This has a serious impact on the normal coal production, deteriorate the conventional anchor bolt support effect, and require the alternative support approaches.

3. Breakthrough solutions for the efficient drivage of roadways at depths over 1 km

3.1. Roadway shape control problems: underbreak and overbreak zones

Fractures induced by conventional blasting methods are very likely to develop from pre-existing fractures in the rock mass, and their propagation direction is highly random and uncertain (Donzé et al., 1997; Ma & An, 2008). This makes it quite difficult to control the fracture direction

of a rock mass and can easily cause excessive overbreak and underbreak (which implies that a roadway perimeter in some places is larger and in others is smaller, respectively, than required by the roadway design). The ensuing problems include inadequate roadway shape, severe loosening of SRR, and a significant decline in the rock mass stability, etc. (Singh & Xavie, 2005; Perras & Diederichs, 2005). A typical configuration of a roadway cross-section with design lines and zones of overbreak and underbreak is shown in Figure 1 (Maerz et al., 1996).

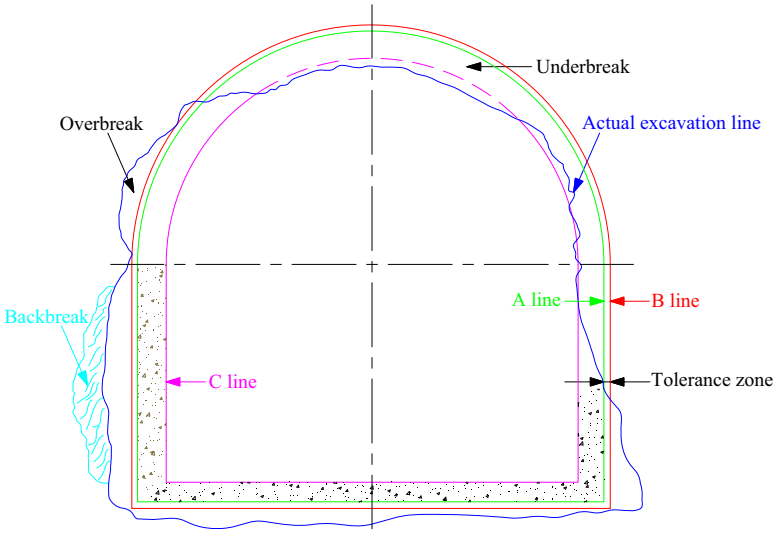

Fig. 1. A roadway cross-section with design lines and typical zones of underbreak and overbreak (Maerz et al., 1996)

Here ‘A line’ is the minimum excavation perimeter, while ‘B line’ is the maximum design parameter, and ‘C line’ is the finished perimeter of a concrete-lined roadway. Underbreak is the rock left inside the A line, which requires a secondary excavation, and backbreak is a special case of overbreak, which is related to the release of geological structure blocks, rather than the blast damage. The tolerance zone is a theoretical space of about 200 mm between A and B lines, which allows for the normal blasthole deviation during the drilling operation. The drilling-and-blasting experience has produced various schemes for arranging the perimeter and secondary blastholes with different layouts. The conventional and improved blasthole layouts for the deep roadways will be discussed in detail in Section 4 of this paper, while the following subsections are dedicated to the improved blasting techniques, which are based on the shaped-charge cumulative jets with the enhanced penetration and directed explosion capabilities.

3.2. Controlled blasting with bidirectional energy focusing for the directional fracturing

To achieve more accurate roadway cross-sectional shape and reduce the number of perimeter holes for more efficient blasthole drilling, a controlled blasting device with bidirectional

energy focusing was designed for the directional fracturing. As shown in Figure 2 (1, V-shaped protrusion; 2, Blasthole; 3, Non-toxic plastic casing; 4, Explosive charge; 5, Energy-focusing cavity; 6, High-velocity and high-pressure jets), this device has two major components: an explosive charge and a non-toxic plastic casing. The non-toxic plastic casing has two V-shaped protrusions on its inner wall, which are symmetrical about its axis. So the cylindrical explosive charge placed into it will be squeezed to form two bidirectional symmetric cavities for focusing of the blast energy, which is similar to the shaped-charge liners in cumulative shells that form armor-piercing high-speed jets. The blasting device for the directional fracturing is then placed into the blastholes drilled along the contour of the roadway to be excavated, with the tips of the cavities being within the plane passing through the hole axes. The blasthole spacing is 1.5 to 2 times longer than that used by the conventional blasting methods. During the explosion, the detonation products in the two energy-focusing cavities (liners) tend to concentrate in the axial direction, creating high-velocity and high-pressure jets. The jets are directly projected onto the wall of each blasthole so that the hole wall will first fracture along the plane passing through the tips of the cavities (Yue et al., 2013). Propelled by the detonation gas, the fracture propagates rapidly and connects the breaches coming from adjacent blastholes. In this way, a smooth fracture plane passing through the blasthole axes will form.

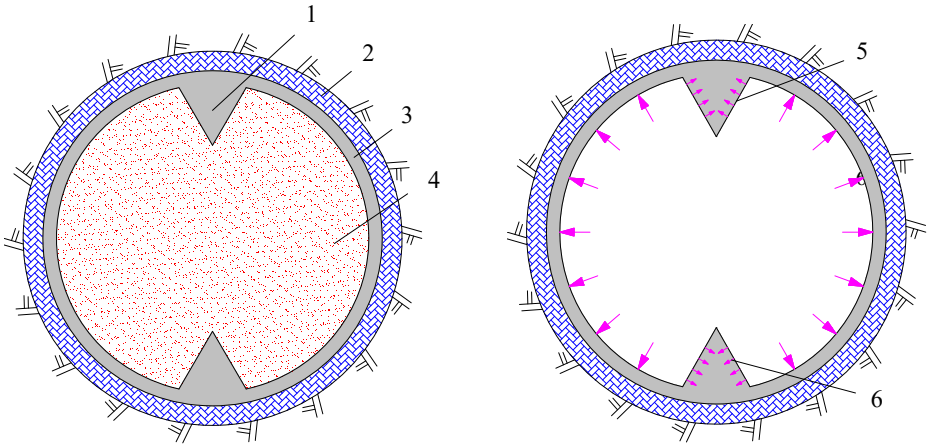

(a) Cross-section of an explosive charge (b) Stress distribution after the explosion

Fig. 2. Schematic of the controlled blasting device for the directional fracturing

The technique of controlled blasting for the directional fracturing has the following advantages: (1) After the explosive charge is detonated, the blast energy will be concentrated in the energy-focusing cavities/liners, and the resulting high-velocity and high-pressure jets will penetrate into the wall rock, creating directional fractures with a dominant direction. The preliminary application of this technique was shown to increase the fracture length by 15-25% and decrease the number of required blastholes and their drilling cost. (2) The preferable fracture propagation in the designed directions impedes the fracture in other directions, thereby increasing the residual half-hole ratio, improving the roadway shape, stabilizing the SRR, and reducing the roadway support cost. (3) The weight of explosive (namely, class 2 emulsion explosive permitted for use

in coal mines) required by the proposed technique is less by over 10% than that of conventional blasting methods. This reduces the vibration and noise caused by blasting and the cumulative damage to the SRR by air blast waves. (4) Given the above findings, this technique can be used as an effective alternative to the available blasting methods, in order to reduce the labor intensity and improve the work efficiency of deep roadway excavations.

3.3. Controlled blasting with multidirectional energy distribution for efficient rock fragmentation

At present, borehole blasting usually utilizes coupled or nearly coupled explosive charges, and the stress waves generated by the explosion can rapidly generate a small crushed zone of an irregular shape around each blasthole (Esen et al., 2003). The crushed zone, despite its small dimensions, can dissipate a large share of the explosive energy. Additionally, this zone obstructs the detonation gas path to the fractures around the blasthole (Far & Wang, 2016), thereby reducing the effective range of rock fragmentation. This, in turn, may cause a number of problems, such as inefficient use of blast energy, high explosive consumption, and excessive cost of driving construction (Xia et al., 2013). To raise the driving efficiency through the rational use of blast energy, a controlled blasting device with multidirectional energy distribution was developed for efficient rock fragmentation. Similar to the previous device, it comprises the explosive charge and plastic casing, as shown in Figure 3 (1, Arc-shaped protrusion; 2, Blasthole; 3, Non-toxic plastic casing; 4, Explosive charge; 5, Energy-distributing cavity; 6, High-velocity and high-pressure jets). The non-toxic plastic casing has six arc-shaped protrusions on its inner wall, which are symmetrical about its axis. After the placement of a cylindrical explosive charge into the casing, the protrusions will act as shaped-charge liners, i.e., multidirectional-energy distributing cavities. When the above blasting device is placed and detonated in the blastholes drilled along the contour of the roadway to be excavated, the blast energy will be concentrated in the energy distributing cavities, generating multidirectional high-velocity and high-pressure jets. The jets

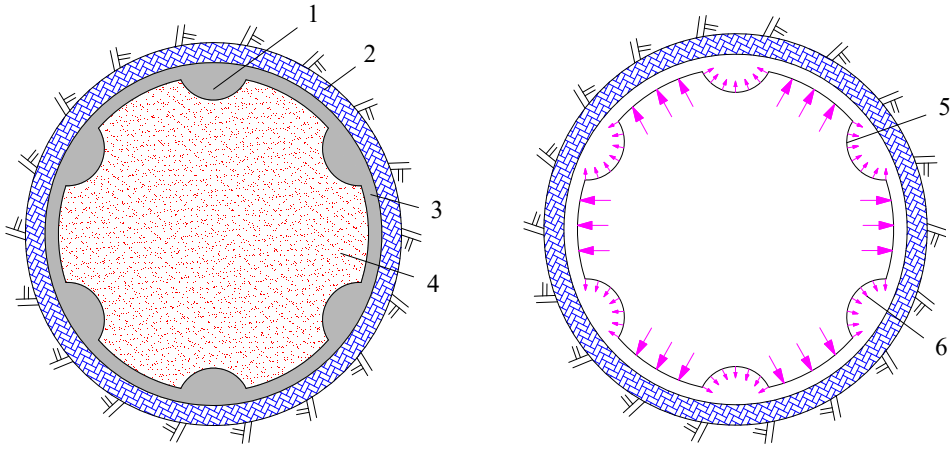

(a) Cross-section of an explosive charge (b) Stress distribution after the explosion

Fig. 3. Schematic of the controlled blasting device for efficient rock fragmentation

then penetrate into the surrounding rock of the blastholes to produce radial fractures in multiple dominant directions, and the detonation gas expansion provides a rapid propagation of these fractures. Additionally, this device can partially convert the blast energy into the jet penetration (Sanchidrian et al., 2007), thus mitigating the hole wall vibration caused by blast waves and effectively preventing the formation of the irregularly shaped crushed zone. In the case of a simultaneous explosion in multiple blastholes, the multidirectional fractures arising from different holes will split the rock into uniformly sized fragments, which substantially improves the efficiency of rock fragmentation and blast energy usage.

The technique of controlled blasting for efficient rock fragmentation has the following advantages: (1) The blasting device improves the efficiency of rock fragmentation through more effective use of the blast energy, as well as allows one to split the rock into uniformly sized fragments and increase the fractured rock volume by 15-20%, as compared to conventional blasting methods. (2) This technique application is more time-saving and labor-effective than conventional ones. (3) The use of the proposed blasting device can reduce the number of required blastholes, thus cutting the consumption of blasting materials and labor intensity. (4) As one detonation needs only a small amount of explosive, the blasting will cause only a limited disturbance to the remaining rock mass. This advantage makes this blasting technique applicable to the excavation in both hard and soft rocks.

3.4. Wedge-cylinder duplex cuts centered on the double empty holes

Insofar as rock masses deeper than 1 km in the XMA are subjected to high compressive stresses before the excavation, blastholes produced by conventional vertical wedge cutting are typically subjected to great clamping forces during blasting (Yuan et al., 2012; Miao et al., 2018), which strongly deteriorates the results. Given this, an innovative technique called 'wedge-cylinder duplex cuts centered on double empty holes' was proposed as a solution to this problem, as shown in Figure 4. This technique combines the advantages of empty holes space, wedge cut, and cylindrical cut, and is suitable for parallel operation with multiple drill rigs. It not only allows one to generate a solid free surface by blasting, but also improves the driving efficiency, increases the cut depth, and ensures the efficient utilization of blastholes. The specific steps involved in the on-site implementation are as follows:

(1) The first step is to drill two empty holes along the vertical symmetry axis of the roadway cross-section to be excavated, according to the locations of cuts designed. The two empty holes can provide a sufficient space to allow for the broken rock expansion that the rock fragments can be rapidly removed. Besides, they can relieve the pressure in the rock mass via the stress re-distribution in the surrounding rock of the empty holes.
(2) Next, first-order wedge cuts are drilled to a relatively shallow depth, with the two empty holes located at the middle of their axis of symmetry. The high applicability, a capacity to concentrate the explosive power, and a large volume of the wedge cut can facilitate the initial free surface formation.
(3) Based on the initial free surface formed by first-order wedge cuts, the second-order cylindrical cuts are drilled to a larger depth with a uniform pattern, to obtain more extensive and deeper cavities of controllable shapes. These cuts provide an excellent free surface for blasting in the auxiliary holes.

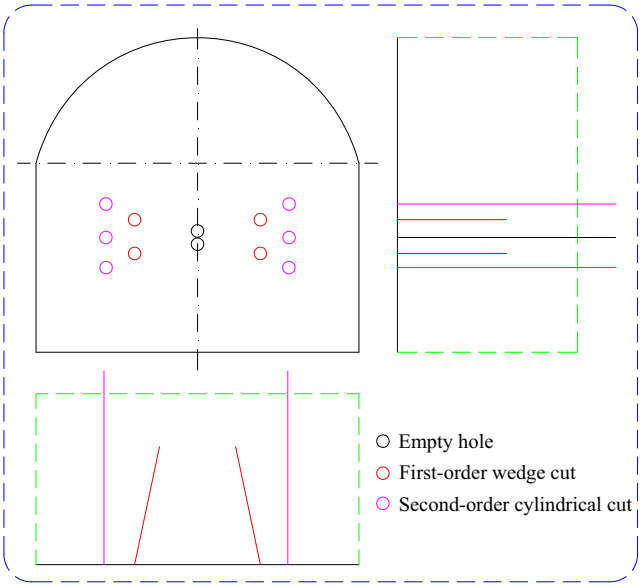

Fig. 4. Schematic of wedge-cylinder duplex cuts centered on double empty holes

3.5. High-strength support techniques for roadways deeper than 1 km

Due to large mining depths and the dominance of horizontal in-situ stresses around roadways deeper than 1 km in the XMA, the SRR tends to undergo large-scale inelastic deformation soon after the roadway excavation. Conventional support methods used for medium-deep roadways are unable to meet the requirements for rock deformation control of roadways deeper than 1 km (Kang et al., 2015; Chang & Xie, 2012). For this reason, a set of high-strength support techniques applicable to roadways below 1 km in the XMA was developed through a survey of geological conditions, a comparative analysis of the advantages and disadvantages of different support methods and their industrial implementations.

(1) Selecting the most proper location and time of the roadway excavation

The first step is to optimize the production sequence and select the proper location of roadway excavation, which is controlled by geomechanical properties of rocks at depths over 1 km in the XMA. It is necessary to avoid areas affected by the dynamic pressure and stress concentration zones as far as possible and to start the construction after the rock pressure stabilization.

(2) Determining a highly adaptable roadway cross-sectional shape

Determining a highly adaptable roadway cross-sectional shape is crucial to achieving effective roadway support. If the immediate roof is broken or the false roof is relatively thick, the roadway can be designed with vertical side walls and a semicircular arch to improve the stress state and bearing capacity of the roof. Such a cross-sectional shape can facilitate effective roadway support and is highly adaptable to such complex geological conditions as deep soft rocks and high in-situ stresses.

(3) High-strength anchor bolts suitable for local mining conditions

Anchor bolts serve primarily to place the rock within the anchorage zone under compression, improve the stress distribution in the interior of SRR, and thereby increase the overall strength and stability of the SRR. Therefore, the strength of anchor bolts is vital in stabilizing the SRR. To adapt to the geological conditions at deep levels in the XMA, two types of high-strength anchor bolts with left-handed threads (designated as KMG600 and BHRB600) were developed for deep roadways in the XMA. Their yield and tensile strength values are as high as 600 and 815 MPa, respectively, which are 30% higher than those of fully threaded anchor bolts.

(4) Grouting anchor cables with high preload

Anchor cables were used to connect the load-bearing structure created by anchor bolts to the interior of the SRR so that the load will be supported by a larger part of the rock mass. This can enhance the overall strength of the SRR. Grouting anchor cables with high preload were developed in combination with the above high-strength anchor bolts. A grouting anchor cable is mainly composed of a pre-stressed anchor head, multiple steel wires (7 mm in diameter), framework, grouting mouth, hollow grouting pipe, and stirrer. The grouting anchor cables range in length from 5 to 8 m and in diameter from 21 to 35 mm. Their breaking load is as high as 600 kN, and preload can reach 250 kN. Besides, specially made high-strength trays were used to assist in the grouting.

(5) New types of thick steel strips for supporting deep roadways

The magnitude of pre-stressing forces applied to the anchor bolts and cables has a strong effect on the effectiveness of roadway support. It is also important to extend the scope of action of pre-stressing forces to more distant parts of the SRR. To deal with the tearing problem of W- and M-shaped steel strips used to support deep roadways in the XMA, two types of more flexible thick steel strips (designated as GRT-M5 and GRT-M6) were developed. Their strength is higher by more than 50% than that of ordinary steel strips. Being jointly used with anchor bolts and cables, these strips can significantly improve the control effect of the SRR.

4. A test implementation of the proposed set of techniques in the particular roadway project

4.1. Selection of blasthole drilling equipment

When constructing a roadway by drilling and blasting, the first operation is blasthole drilling. Efficiency of rock drilling largely determines the speed of subsequent construction (Zhang et al., 2018). During drilling at a depth over 1 km, the drill rods are usually subjected to the action of large clamping forces due to the high horizontal stress and high rock hardness. This hinders the performance of conventional pneumatic drills in cutting of blastholes. To achieve efficient excavation of deep roadways in this area, a fully hydraulic drilling jumbo with crawler (CMJ17HT, Huatai Mining & Metallurgical Machinery Company, Zhangjiakou, China) was used to drill blastholes. The CMJ17HT drilling jumbo has multiple advantages as follows.

(1) The fully hydraulic double-armed drilling system enables a rapid and efficient drilling. For the given rock type and hole diameter, its drilling speed is more than twice faster than that of a pneumatic drill rig.

(2) Its drilling mechanism allows for the fullface driving and its impact-induced stress waves are less pronounced. Being combined with the drill rod high efficiency in transmitting the torque, the cost of drilling tools is cut by 15-20%.
(3) The modular design of this jumbo contributes to higher operational stability, lower probability of mechanical failure, lower operational noise, and higher gradeability, thereby significantly improving the construction efficiency and quality.

Noteworthy is that during drilling, workers could stay away from the driving face end, in order to avoid the operation under unsupported roof and protect their safety. Table 2 presents the operating parameters of the CMJ17HT drilling jumbo, while its photos are presented in Figure 5.

TABLE 2

Operating parameters of the CMJ17HT drilling jumbo

Operating parameters	Units	Desired values
Dimensions during operation (Length × Width × Height)	mm	7500 × 1160 × 1750
Weight	kg	8800
Crawler width	mm	350
Number of drill arms		2
Permissible cross-sectional area	m^2	4-23
Travel speed	m/min	0-40
passable gradient	°	0-14
Impact frequency	Hz	33-60
Rated torque	N·m	220
Rated rotational speed	r/min	200
Thrust force	N	7000
Drilling speed	m/min	0.8-2
Hole diameter	mm	27-42
Hole depth	m	2.6

(a) Assembly state (b) Operation state

Fig. 5. Photos of the CMJ17HT drilling jumbo

4.2. Analysis of experimental results

(1) Overview of the exploratory roadway

Buried at a depth of 1,130 m, the –1010 WRR at the HCM, XMA, is a typical roadway excavated at a depth over 1 km and in high in-situ stress conditions. It has a design length of 927 m and a slope of 5‰. Its gross and net cross-sectional areas are 15.76 and 13.74 m^2, respectively. The roadway construction process included the following steps: 1) Cutting blast holes using the CMJ17HT drilling jumbo; 2) Loading the blastholes with the explosive charge and detonating the explosive; 3) Providing temporary support to the roadway; 4) Removing waste rock from the excavation using the side dumping loader (ZC-3B, Shandong China Coal Industrial Supply Company, Jining, China); 5) Transporting using the shuttle car (ST-14/6B, Shandong Zhuoli Mining Equipment Company, Jining, China); and 6) Providing the permanent roadway support.

(2) Analysis of blasting results

Figure 6 depicts the blasthole layout parameters in the original design for the construction of –1010 WRR by drilling and blasting at the HCM. The blasting parameters of the original design are listed in table 3 (HT, hole type; HS, hole spacing; WPH, weight per hole; NHs, number of holes; TW, total weight; BO, blasting order; SL, stemming length; NSPs, number of stemming plugs; CH, cut hole; AH, auxiliary hole; SLH, second-lap hole; PH, periphery hole; BH, bottom hole; RHL, remaining hole length). However, the original design failed to provide the desired results. In the industrial implementation, the controlled blasting device with the bidirectional energy focusing was employed to control the shaping of periphery holes, and then the controlled blasting device with the multidirectional energy distribution was used to load the blastholes with explosive charges. Moreover, the wedge cuts in the original design were changed to wedge-cylinder duplex cuts centered on the double empty holes. The blasthole layout parameters were further optimized by reducing the number of blastholes from 72 in the original design to 61. The blasthole layout parameters after the optimization are illustrated in Figure 7 and the blasting parameters after the optimization in table 4 (EH, empty hole; FOCH, first-order cut hole; SOCH, second-order cut hole). After drilling, a class 2 emulsion explosive permitted for use in coal mines and 1-5 millisecond delay detonators were loaded into each blasthole, with the detonator placed closer to the hole mouth. The detonators in all blastholes were connected in series and ignited using an exploder (MFB-200, Shandong Ouke Machinery Equipment Company, Jining, China). During the construction, full cross-section loading and blasting were carried out. The desired goals, including long advance, high efficiency, weak disturbance, and small underbreak and overbreak, were achieved, demonstrating excellent results.

1) The depth of blastholes drilled by the CMJ17HT drilling jumbo was 2,500 mm, as compared to the 1,700 mm length of blastholes drilled by the conventional pneumatic drill rig. The driving efficiency was significantly improved, with the advance of working cycle reaching 2,300-2,400 mm. The average and maximum monthly advances were 125 and 151 m, respectively, which implied a substantial increase in the advance rate.
2) The drilling via wedge-cylinder duplex cuts centered on double empty holes significantly increased the effective depths of cuts. The problem of the low utilization rate of blastholes was addressed, the utilization rate of blastholes reached over 95%, which was 15% higher than that obtained using the original design.

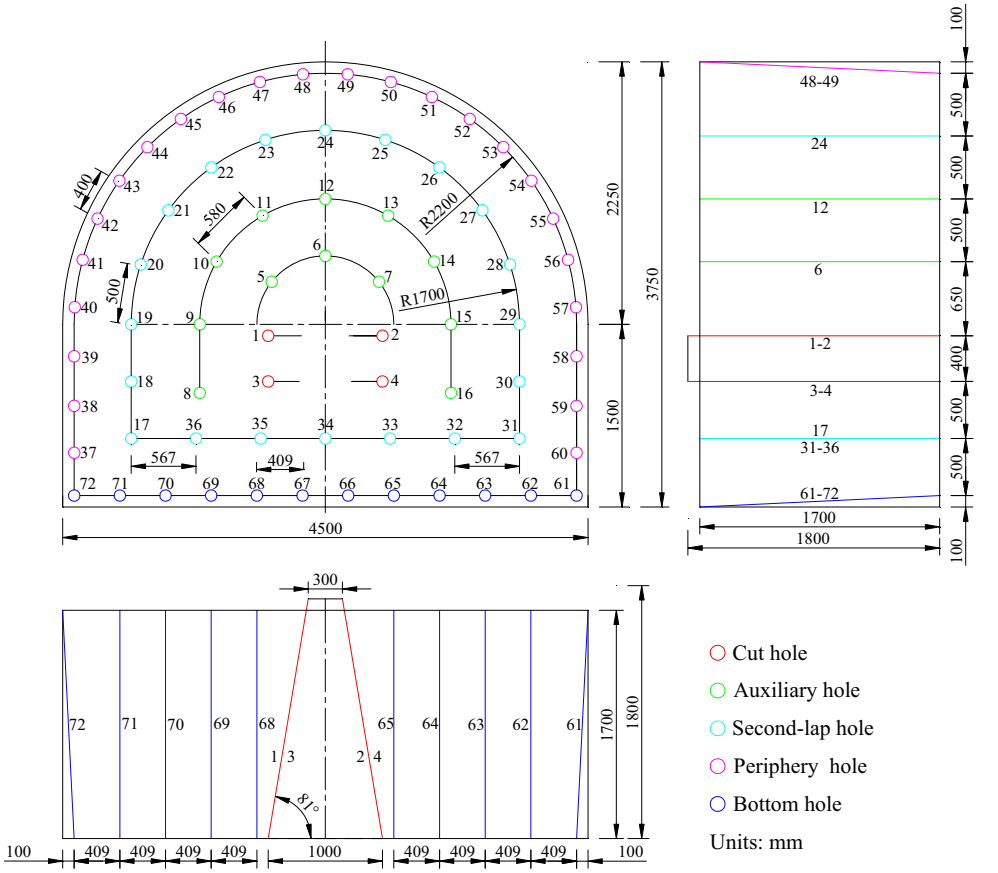

Fig. 6. Blasthole layout parameters in the original design

TABLE 3

Blasting parameters in the original design

HT	No.	Depth/m	HS/m	Angle/°		Explosive charge			BO	SL	NSPs
				Horizontal	Vertical	WPH/kg	NHs	TW/kg			
CH	1-4	1.8	1.0/0.4	81	90	0.6	4	2.4	1	RHL	4
AH	5-16	1.7	0.58	90	90	0.45	12	5.4	2		12
SLH	17-36	1.7	0.5	90	90	0.45	20	9	3		20
PH	37-60	1.7	0.4	90/87	87/90	0.3	24	5.4	4		24
BH	61-72	1.7	0.409	90	87	0.6	12	7.2	5		12

3) The use of the proposed two controlled blasting techniques led to a 50%-increase in the perimeter hole spacing, a 15%-increase in the residual half-hole ratio, and a reduction in the number of blastholes, thereby saving the time required for the rock drilling.
4) Cracks induced by blast waves were rarely observed during the construction, indicating a significantly improved quality of blasting. The size of rock fragments produced by blast-

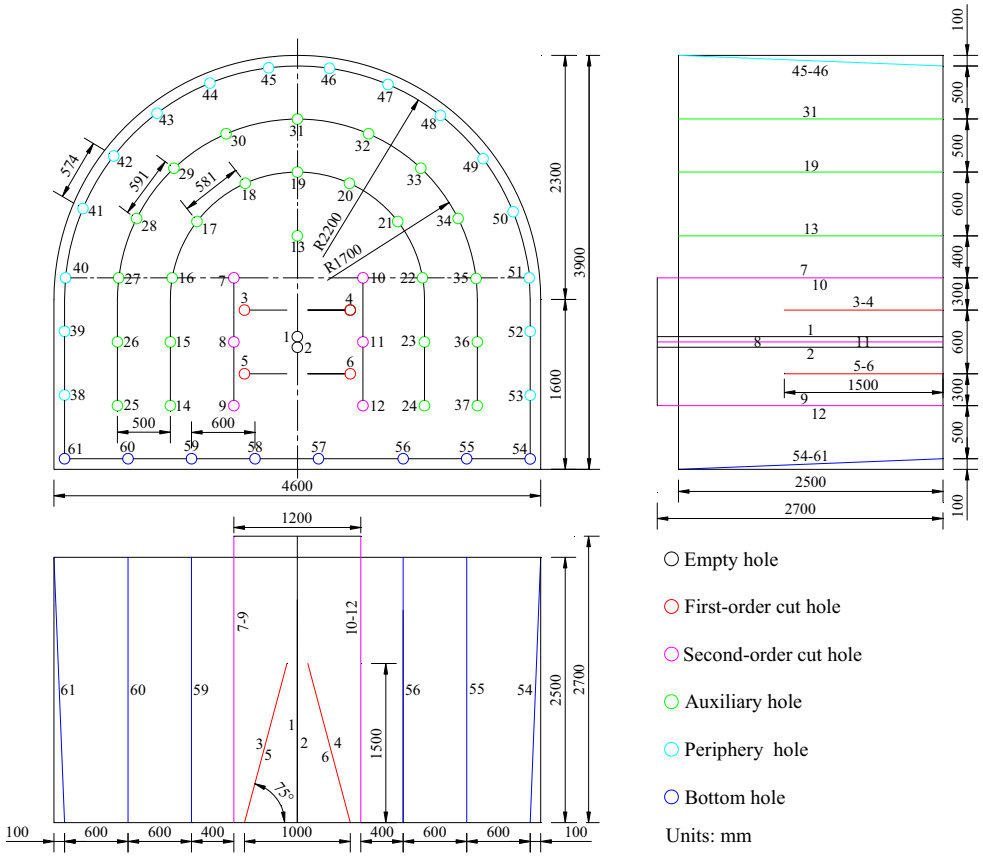

Fig. 7. Blasthole layout parameters after the optimization

TABLE 4

Blasting parameters after the optimization

HT	No.	Depth/m	HS/m	Angle/°		Explosive charge			BO	SL	NSPs
				Horizontal	Vertical	WPH/kg	NHs	TW/kg			
EH	1-2	2.7	/	90	90	0.3	2	0.6	1	RHL	/
FOCH	3-6	1.5	1	75	90	0.6	4	2.4	1		4
SOCH	7-12	2.7	1.2	90	90	0.9	6	5.4	2		6
AH	13-37	2.5	0.6	90	90	0.6	25	15	3		25
PH	38-53	2.5	0.6	90/87	87/90	0.45	16	7.2	4		16
BH	54-61	2.5	0.6	90	87	0.75	8	6	5		8

ing ranged from 10 to 30 mm and the muck piles were relatively closely spaced, allowing more efficient loading and transportation of rock.

5) Damage to the SRR was substantially diminished, and the overbreak and underbreak zones were within 50 mm, facilitating the subsequent support measures.

3) Analysis of the effectiveness of roadway supports

The –1010 WRR at the HCM penetrated through the strata lying between $\#7_{(1)}$ and $\#8_{(1)}$ coal seams. The SRR is mostly siltstone and fine-grained sandstone, with an occasional appearance of marlite. To avoid the repeated maintenance during service, high-strength pre-stressed anchor bolts and cables were used in combination with shotcrete and grout to provide a primary permanent support to the WRR. The full cross-section support configuration parameters are shown in Figure 8.

1) Roof and sidewall supports

The roof and two sidewalls of the WRR were supported with BHRB600 high-strength anchor bolts. With a diameter of 22 mm and length of 2.4 m, this bolt type features left-handed threads, M27 thread on bolt tail, and no longitudinal ribs. Bolts were arranged at intervals of 800 mm in rows. Adjacent rows were spaced 800 mm apart, and each row had 13 bolts. The sidewall bolts near the floor were installed at an angle of 30° to the vertical line. The pre-load designed for the bolts was 170 kN. A new type of high-strength anchoring agent (Z2835) was used to anchor the bolts by the full-length anchorage (two pieces per bolt). Accessories used included M27×3 high-strength nuts for the bolts, GRT-M5 thick steel strips, high-strength tray (150 mm × 150 mm × 12 mm) with a bearing capacity no lower than 400 kN. Reinforcing meshes made of cold drawn steel wires (6.5 mm in diameter) were used to stabilize the roadway surface. Each mesh had dimensions of 5.0 m × 0.9 m and a grid size of 0.1 m × 0.1 m. The trays were used to press the wire meshes firmly against the rock surface. The exposed length of the bolts ranged from 30 to 50 mm. High-strength pre-stressed grouting anchor cables were installed along the roof midline. The cables were 22 mm in diameter and 5.3 m in length. Their row spacing was 900 mm. The cables were anchored using two resin anchoring agents (K2550 and M2575), with the extended anchorage segment. The cables were attached to high-strength trays with an adjustable core having dimensions of 300 mm × 300 mm × 16 mm with the help of the accompanying lock. A grouting hole of 18 mm diameter was made in each tray. A pre-load of 300 kN was designed for the cables.

2) Floor support

The floor of the WRR was also stabilized with anchor bolts and accessories used for the roof and sidewalls. The floor bolts were arranged in rows spaced 800 mm apart, and each row had three bolts spaced 1.1 m apart.

3) Shotcrete lining support

After the blasting-induced excavation, a 30 mm-thick concrete layer was sprayed onto the rock surface to offer a temporary support and leveling up the localized overbreak zones. After the anchor bolts and cables for the roof were installed in place, the floor lifting and rock bolting for the two sidewalls and the floor were carried out. Next, the concrete was sprayed repeatedly onto the rock surface until the shotcrete lining thickness reached 70 mm.

4) Reinforced support by grouting

During the driving process, grout was injected into the broken SRR for the reinforced support. The grouting process involved the following steps. Firstly, a counterbore with a 56 mm diameter and 500 mm depth was cut at the orifice of each roof anchor cable. Steel tubes with a diameter of 100 mm and a length of 2.4 m were used as grouting anchor bolts for the floor. They were installed in rows spaced 1.5 m apart, two tubes per row. Then, the #525 ordinary Portland cement with sodium silicate addition was used as the grout, and the grouting pressure was maintained at about 3 MPa.

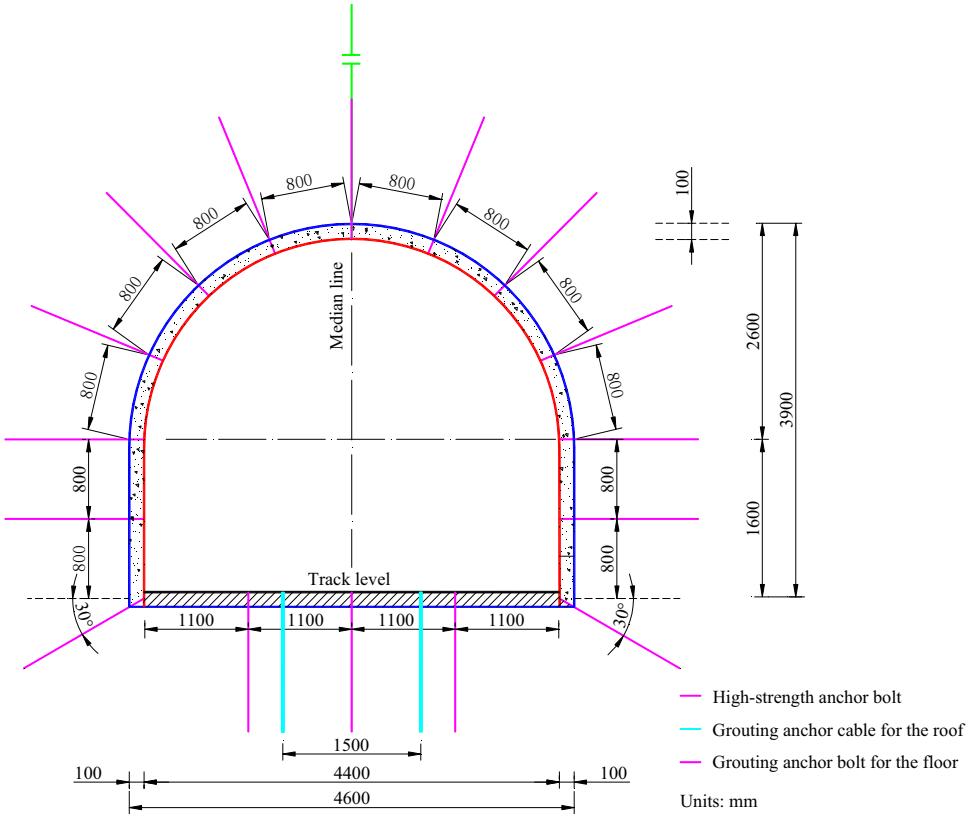

Fig. 8. Schematic of the support scheme for the –1010 WRR

After the –1010 WRR was excavated, a deformation observation station was set up halfway along its length (450 m ahead of the starting point). The deformation of the SRR was then assessed using cross measurements, to examine the actual effectiveness of supports. The results obtained indicated that the maximum roof-to-floor convergence was about 160 mm, while the maximum convergence of the two sidewalls was about 75 mm. The maximum roof subsidence was 100 mm, and the maximum floor heave was 80 mm. The surface deformation of the SRR became stable after about 45 days. To obtain the deformation and failure of the interior part of the SRR, an imaging instrument (TYGD10, Jiangsu Huidun Mining Science Company, Xuzhou, China) was placed into the boreholes (56 mm in diameter and 6.0 m in depth) drilled at the observation station. The images obtained in Figure 9 revealed that the interior SRR maintained a high structural integrity with no apparent signs of bed separation, sliding, fracture propagation, development of new fractures or other deformation features, except for the small horizontal cracks located 4.0 m from the borehole mouth from the left sidewall in Figure 9(b). The results of surface displacement monitoring, together with the borehole observations, strongly suggested that the deformation of the SRR was adequately controlled in Figure 10. This confirms that the support scheme and parameters adopted are reasonable and feasible, can ensure safe underground mining, and minimize the repeated maintenance and repair costs.

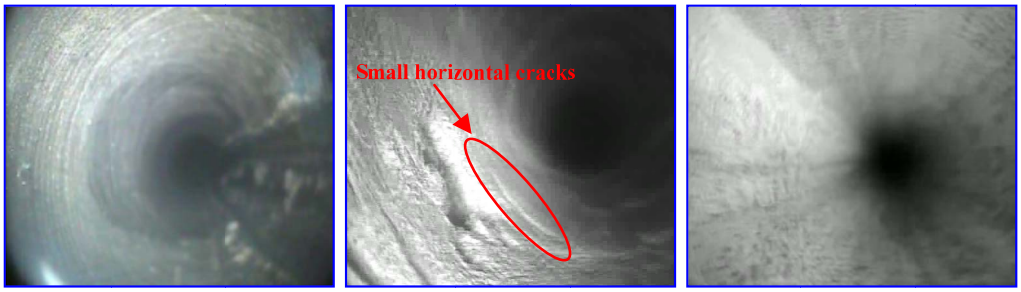

(a) 5.5 m from the roof surface (b) 4.0 m from the left sidewall surface (c) 3.0 m below the floor surface

Fig. 9. Images of boreholes drilled in the SRR

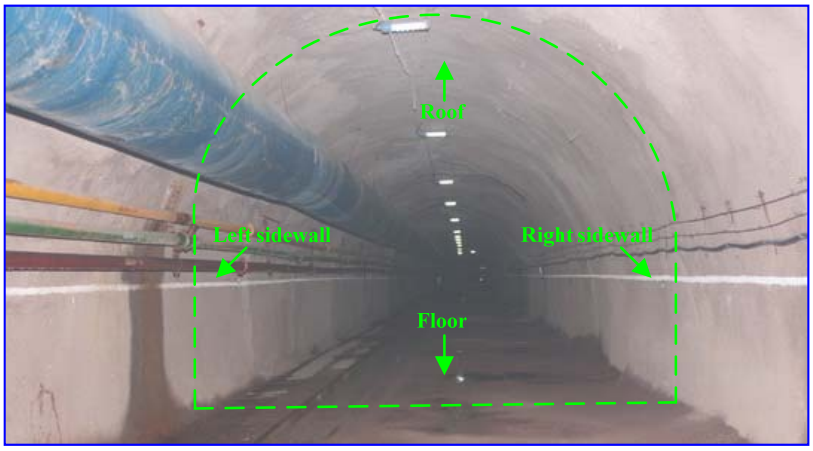

Fig. 10. Actual shaping effect of –1010 WRR

5. Conclusion

(1) The in-situ stress measurements in roadways deeper than 1 km in the XMA, strongly indicate that the prevailing in-situ stresses are horizontal ones, which pattern is characteristic of a tectonic stress field. Based on this, a set of techniques for efficiently driving roadways at depths over 1 km was developed, including the controlled blasting with bidirectional energy focusing for directional fracturing, controlled blasting with multidirectional energy distribution for efficient rock fragmentation, wedge-cylinder duplex cuts centered on double empty holes, and high-strength supports for roadways deeper than 1 km.

(2) On the basis of the state-of-the-art shaped-charge blasting theory, fracture mechanics, and rock mechanics, two controlled blasting devices were developed: one with bidirectional energy focusing ability and the other with multidirectional energy distribution capacity. The joint application of these devices made it possible to achieve the directional fracturing of the SRR, improve the cross-sectional shape of the roadway, reduce the

number of blastholes and the explosive consumption, as well as improve the drilling and blasting efficiency.

(3) To overcome the shortcomings of conventional vertical wedge cut, the wedge-cylinder duplex cuts centered on double empty holes were proposed. This technique is suitable for the parallel operation with multiple drill rigs. It can not only generate a solid free surface by blasting but also improve the construction efficiency of roadway drivage, increase the cut depth, and ensure the efficient utilization of blastholes.

(4) A set of high-strength support techniques adapted to the local geological conditions was developed for roadways deeper than 1 km in the XMA. These support techniques involve the selection of the most proper location and time of roadway excavation, determining a highly adaptable roadway cross-sectional shape, and using high-strength anchor bolts suitable for the local mining conditions, grouting anchor cables with high preload, and new types of thick steel strips for supporting deep roadways.

(5) The industrial implementation results indicate that rapid construction progress was achieved by use of the proposed set of innovative techniques. The average and maximum monthly advances were 150 m and 151 m, respectively. Moreover, the maximal deformation levels of the SRR fell within the allowable ranges (maximum roof-to-floor convergence of 160 mm; maximum convergence of the two sidewalls of about 75 mm; maximum roof subsidence of 100 mm; and maximum floor heave of 80 mm). The surface and interior of the SRR exhibited no significant deformation or failure, confirming that the support scheme and parameters are reasonable and feasible and can ensure safe underground mining and avoid the repeated maintenance and repair.

(6) Compared with the other excavation methods of roadway depths over 1 km, these novel techniques can better enhance the stability of SRR, and reduce the blasting disturbance to the retained rock mass, thus improving the reliability and safety of roadway excavation. The presented innovative method is well targeted and highly adaptable, it is suitable to both hard rock roadways and soft rock roadways. But it must be pointed out that the relevant technical parameters need to be modified according to the practical conditions of the roadways. Relevant findings of this study are expected to provide a technical guidance for the efficient driving of roadways at depths over 1 km in other mining areas.

Acknowledgments

We acknowledge the financial support for this work provided by the Fundamental Research Funds for the Central Universities (No. 2017XKQY022). We wish to thank the HCM of the XMA in Shandong province, China, for supporting to conduct this important study. We are also grateful to Mapletrans Company in Wuhan, China, for its professional English editing service. Special thanks are given to the anonymous reviewers for their constructive comments and helpful suggestions.

References

Agliardi F., Crosta G., Zanchi A., 2001. *Structural constraints on deep-seated slope deformation kinematics.* Engineering Geology **59**, 1, 83-102.

Blondeel M., Van de Graaf T., 2018. *Toward a global coal mining moratorium? A comparative analysis of coal mining policies in the USA, China, India and Australia.* Climatic Change **150**, 1-2, 89-101.

Cai M., 2011. *Rock mass characterization and rock property variability considerations for tunnel and cavern design.* Rock Mechanics and Rock Engineering **44**, 4, 379-399.

Cai M.F., Peng H., 2011. *Advance of in-situ stress measurement in China.* Journal of Rock Mechanics and Geotechnical Engineering **3**, 4, 373-384.

Chang J.C., Xie G.X., 2009. *Mechanical characteristics and stability control of rock roadway surrounding rock in deep mine.* Journal of China Coal Society **34**, 7, 881-886.

Chang J.C., Xie G.X., 2012. *Research on space-time coupling action laws of anchor-cable strengthening supporting for rock roadway in deep coal mine.* Journal of Coal Science and Engineering **18**, 2, 113-117.

Chen S.D., Tang D.Z., Tao S., Xu H., Li S., Zhao J.L., Ren P.F., Fu H.J., 2017. *In-situ stress measurements and stress distribution characteristics of coal reservoirs in major coalfields in China: Implication for coalbed methane (CBM) development.* International Journal of Coal Geology **182**, 1, 66-84.

Diering D.H., 1997. *Ultra-deep level mining – future requirements.* Journal of the South African Institute of Mining and Metallurgy **97**, 6, 249-255.

Donzé F.V., Bouchez J., Magnier S.A., 1997. *Modeling fractures in rock blasting.* International Journal of Rock Mechanics and Mining Sciences **34**, 8, 1153-1163.

Esen S., Onederra I., Bilgin H.A., 2003. *Modelling the size of the crushed zone around a blasthole.* International Journal of Rock Mechanics and Mining Sciences **40**, 4, 485-495.

Fairhurst C., 2017. *Some challenges of deep mining.* Engineering **3**, 4, 527-537.

Far M.S., Wang Y., 2016. *Probabilistic analysis of crushed zone for rock blasting.* Computers and Geotechnics **80**, 1, 290-300.

He M.C., Xie H.P., Peng S.P., Jiang Y.D., 2005. *Study on rock mechanics in deep mining engineering.* Chinese Journal of Rock Mechanics and Engineering **24**, 16, 2803-2813.

Huang X., Liu Q.S., Shi K., Pan Y.C., Liu J.P., 2018. *Application and prospect of hard rock TBM for deep roadway construction in coal mines.* Tunnelling and Underground Space Technology **73**, 1, 105-126.

Hu W.Y., Dong S.N., 2008. *Research on the sudden changes and the controlling factors of deep coal mining conditions.* International Journal of Coal Science and Technology **14**, 3, 347-351.

Kang H.P., Fan M.J., Gao F.Q., Zhang H., 2015. *Deformation and support of rock roadway at depth more than 1000 meters*. Chinese Journal of Rock Mechanics and Engineering **34**, 11, 2227-2241.

Kang H.P., Lin J., Zhang X., 2007. *Research and application of in-situ stress measurement in deep mines.* Chinese Journal of Rock Mechanics and Engineering **26**, 5, 929-933.

Kang H.P., 2014. *Support technologies for deep and complex roadways in underground coal mines: A review.* International Journal of Coal Science & Technology **1**, 3, 261-277.

Kang H.P., Zhang X., Si L.P., Wu Y., Gao F., 2010. *In-situ stress measurements and stress distribution characteristics in underground coal mines in China.* Engineering Geology **116**, 3-4, 333-345.

Kang Y.S., Liu Q.S., Xi H.L., 2014. *Numerical analysis of THM coupling of a deeply buried roadway passing through composite strata and dense faults in a coal mine.* Bulletin of Engineering Geology and the Environment **73**, 1, 77-86.

Kulatilake P.H.S.W., Wu Q., Yu Z.X., Jiang F.X., 2013. *Investigation of stability of a tunnel in a deep coal mine in China.* International Journal of Mining Science and Technology **23**, 4, 579-589.

Lavrov A., 2003. *The Kaiser effect in rocks: principles and stress estimation techniques.* International Journal of Rock Mechanics and Mining Sciences **40**, 2, 151-171.

Li S.C., Wang Q., Wang H.T., Jiang B., Wang D.C., Zhang B., Li Y., Ruan G.Q., 2015. *Model test study on surrounding rock deformation and failure mechanisms of deep roadways with thick top coal.* Tunnelling and Underground Space Technology **47**, 1, 52-63.

Li X.L., Hu H., He L.H., Li K.G., 2017. *An analytical study of blasting vibration using deep mining and drivage rules.* Cluster Computing **20**, 1, 109-120.

Luo Y., Yuan L., Yang Y., 2014. *Experimental study on stability control technology of surrounding rock of deep roadways in coal mine.* Engineering Sciences **12**, 2, 12-21.

Maerz N.H., Ibarra J.A., Franklin J.A., 1996. *Overbreak and underbreak in underground openings part 1: measurement using the light sectioning method and digital image processing.* Geotechnical and Geological Engineering **14**, 4, 307-323.

Ma G.W., An X.M., 2008. *Numerical simulation of blasting-induced rock fractures.* International Journal of Rock Mechanics and Mining Sciences **45**, 6, 966-975.

Malan D.F., Basson F.R.P., 1998. *Ultra-deep mining: The increased potential for squeezing conditions.* Journal of the South African Institute of Mining and Metallurgy **98**, 7, 353-363.

Ma L.Q., Zhang D.S., Zhou M., Qiu X.X., 2009. *Allocation of mechanized operation line for rapid heading of large cross-section rock roadway in deep mine.* Coal Science and Technology **37**, 8, 73-77.

Martin C.D., Kaiser P.K., Christiansson R., 2003. *Stress, instability and design of underground excavations.* International Journal of Rock Mechanics and Mining Sciences **40**, 7-8, 1027-1047.

Miao Y.S., Li X.J., Yan H.H., Wang X.H., Sun J.P., 2018. *Research and application of a symmetric bilinear initiation system in rock blasting.* International Journal of Rock Mechanics and Mining Sciences **102**, 1, 52-56.

Perras M.A., Diederichs M.S., 2016. *Predicting excavation damage zone depths in brittle rocks.* Journal of Rock Mechanics and Geotechnical Engineering **8**, 1, 60-74.

Qi C.Z., Qian Q.H., Wang M.Y., 2009. *Evolution of the deformation and fracturing in rock masses near deep-level tunnels.* Journal of Mining Science **45**, 2, 112-119.

Qi Y., Stern N., Wu T., Lu J.Q., Green F., 2016. *China's post-coal growth.* Nature Geoscience **9**, 8, 564-566.

Ranjith P.G., Zhao J., Ju M.H., Silva R.V.S., Rathnaweera T.D., Bandara A.K.M.S., 2017. *Opportunities and challenges in deep mining: A brief review.* Engineering **3**, 4, 546-551.

Rautenstrauch O., Kulassek M., 2014. *Equipment for underground roadway drivage: Products and engineering from Neuhäuser GmbH.* Mining Report **150**, 4, 228-233.

Sanchidrian J.A., Segarra P., Lopez L.M., 2007. *Energy components in rock blasting.* International Journal of Rock Mechanics and Mining Sciences **44**, 1, 130-147.

Sasmito A.P., Birgersson E., Ly H.C., Mujumdar A.S., 2013. *Some approaches to improve ventilation system in underground coal mines environment – A computational fluid dynamic study.* Tunnelling and Underground Space Technology **34**, 1, 82-95.

Sato T., Kikuchi T., Sugihara K., 2000. *In-situ experiments on an excavation disturbed zone induced by mechanical excavation in Neogene sedimentary rock at Tono mine, central Japan.* Engineering Geology **56**, 1-2, 97-108.

Singh S.P., Xavier P., 2005. *Causes, impact and control of overbreak in underground excavations.* Tunnelling and Underground Space Technology **20**, 1, 63-71.

Xia X., Li H.B., Li J.C., Liu B., Yu C., 2013. *A case study on rock damage prediction and control method for underground tunnels subjected to adjacent excavation blasting.* Tunnelling and Underground Space Technology **35**, 1, 1-7.

Yang R.S., 2013. *Present status and outlook on safety and high efficient heading technology of mine rock roadway in China.* Coal Science and Technology **41**, 9, 18-23.

Yuan W.H., Ma Q.Y., Huang W., 2012. *Model experiment and analysis of wedge-shaped cutting millisecond blasting.* Chinese Journal of Rock Mechanics and Engineering **31**, S1, 3352-3356.

Yue Z.W., Yang L.Y., Wang Y.B., 2013. *Experimental study of crack propagation in polymethyl methacrylate material with double holes under the directional controlled blasting.* Fatigue & Fracture of Engineering Materials & Structures **36**, 8, 827-833.

Zhang J.G., 2017. *Mining-induced stress characteristics and fracture evolution law of over one kilometer deep Pingdingshan coal mine.* Journal of China University of Mining & Technology **46**, 5, 1041-1049.

Zhang W., Li P., Zhang D.S., Yang Z., 2018. *A novel clean mining technology involving the underground disposal of waste rock in coal mines*. Archives of Mining Sciences **63**, 1, 83-98.

Zhang W., Zhang D.S., Shao P., Wang X.F., 2011. *Fast drilling and blasting construction technology for deep high stress rock roadway.* Journal of China Coal Society **36**, 1, 43-48.

Zhang Z.R., Guo Y.X., Jiao W.G., Tong W.J., 2018. *Study on high efficient and rapid construction technology of drilling and blasting method in bedrock section of large section inclined shaft.* Coal Science and Technology **46**, 2, 126-130.

Zheng Y.L., Zhang Q.B., Zhao J., 2016. *Challenges and opportunities of using tunnel boring machines in mining.* Tunnelling and Underground Space Technology **57**, 1, 287-299.